Chapter V. Assembly of an artificial protein hydrogel through leucine zipper aggregation and disulfide bond formation

Abstract

We present a strategy to stabilize artificial protein hydrogels through covalent bond formation following physical association of terminal leucine zipper domains. Artificial proteins consisting of two terminal leucine zipper domains and a random coil central domain form transient networks above a certain concentration, but the networks dissolve when placed in excess buffer. Engineering of a cysteine residue into each leucine zipper domain allows formation of disulfide bonds templated by leucine zipper aggregation. Circular dichroism spectra show that the zipper domains remain helical after cysteine residues and disulfide bonds are introduced. Asymmetric placement of the cysteine residues in the leucine zipper domains suppresses intramolecular disulfide bonds and creates linked "multichains" composed of ca. 9 protein chains on average, as determined by multiangle light scattering measurements. These "multichains" act as the building units of the physical network formed by leucine zipper aggregation. The increased valency of the building units stabilizes the hydrogels in open solutions, while the physical nature of their association allows the reversibility of gelation to be retained. The gel networks dissolve at pH 12.2, where the helicity of the leucine zipper domains is reduced by ca. 90%, and re-form upon acidification. The hydrogels show anisotropic swelling when anchored on aminated surfaces, and may find applications in tissue engineering, controlled release and microarray technologies on the basis of their stability, reversibility and swelling behavior.

1. Introduction

Hydrogels have attracted interest over many years, in part for fundamental reasons and in part because of their potential for application in fields ranging from superabsorbents to tissue engineering[1-9]. Hydrogels are chemically or physically crosslinked networks that absorb substantial amounts of aqueous solutions. They are especially interesting as candidate materials for tissue engineering, because the high water content of the network can be matched to that of soft tissue[9]. Hydrogels currently used in biomedical engineering are prepared from either natural or synthetic polymers[1]. Hydrogel-forming natural polymers include proteins such as collagen and gelatin, and polysaccharides such as alginate and agarose. These materials exhibit useful properties[1], but sources are limited, properties are variable, and concerns about viral contamination restrict the use of animal products in biomedical applications. Systematic control of structure and properties is also difficult. On the other hand, synthetic polymers address these shortcomings at the expense of specific biological functionality.

With genetically engineered biopolymers, it is possible to combine the advantages of both classes. Hydrogels constructed from genetically engineered self-assembling proteins have been prepared in our laboratory[10] and by others[11]. The artificial proteins reported by our laboratory, here designated as $AC_{10}A$, are multidomain proteins consisting of two associative leucine zipper end-blocks (A) and a random coil midblock (C_{10}) (Scheme 1). Leucine zippers constitute a subcategory of coiled-coil domains found widely in nature, and play critical roles in functions ranging from muscle contraction[12] to transcriptional control[13]. Coiled-coils are characterized by heptad repeating units designated as *abcdefg*, where the *a* and *d* positions are occupied by hydrophobic residues

such as leucine, and the *e* and *g* positions are occupied by charged residues. These domains fold into amphiphilic α-helices, and hydrophobic interactions drive association into oligomeric clusters[14]. Self-assembly of the leucine zipper domains of the $AC_{10}A$ protein leads to a network, in which oligomer bundles serve as junction points[10]. These hydrogels are reversible in response to pH and temperature. The physically associated network can be turned off under conditions of high pH or high temperature, where the leucine zipper domains are denatured[10]. The hydrophilic midblock lacks regular secondary structure and prevents precipitation of the chain under conditions that favor leucine zipper aggregation.

Artificial proteins such as $AC_{10}A$ are readily prepared by biosynthetic methods. The amino acid sequence of interest is encoded into an artificial gene, and the protein is expressed in an appropriately transformed bacterial host. The flexibility of recombinant DNA technology allows systematic investigation of structure-property relationships, and provides the potential for incorporating biological information—including cell binding domains and enzyme recognition sites—into engineered hydrogels. Since gelation is driven by self-assembly of protein domains and does not require chemical crosslinking reagents, cytotoxicity of these hydrogels is low. The low cytotoxicity of $AC_{10}A$ was established by a WST-1 assay[15] on 3T3 fibroblast cells cultured in the presence of $AC_{10}A$ (discussed in Chapter VI).

$AC_{10}A$ forms transient networks above a threshold concentration, as manifested by a plateau in the storage modulus in the high frequency regime in dynamic rheological tests. However, these hydrogels dissolve quickly when placed in open solutions near

physiological pH. This behavior precludes their use in applications in which the gel is surrounded by excess water or tissue fluid.

Here we present a successful strategy to improve the stability of artificial leucine zipper hydrogels in open systems. We show that dissolution can be suppressed by judicious engineering of disulfide bonds between leucine zipper domains. The combined effects of leucine zipper self-assembly and disulfide bonding result in artificial protein hydrogels that are stable in open solutions near physiological pH and reversible in response to pH in closed systems.

2. Design considerations

Dissolution of $AC_{10}A$ hydrogels is a consequence of the structural and dynamic properties of leucine zipper aggregates and of the topological states of the artificial protein chains. The small aggregation number of leucine zipper assemblies (discussed in Chapter II), the constant exchange of the constituent peptides (discussed in Chapter III), and the tendency of the protein to form loops (discussed in Chapter II), are all significant factors. Unlike the hydrophobic alkyl endgroups of synthetic associative polymers[16], the leucine zipper domains of $AC_{10}A$ are characterized by small aggregation numbers. Kennedy[17] found that such leucine zipper domains oligomerize into dimers and tetramers at micromolar concentrations; at the higher concentrations where hydrogels form, tetramers dominate. Oligomeric leucine zipper aggregates are known to undergo rapid strand exchange[18,19]. The topological states of the protein chains are also critical. When the two endgroups of a given chain participate in different network junctions, the midblock of the chain forms a bridge. When both ends participate in the same junction,

the chain forms a loop and does not contribute to the elasticity of the network. Rheological measurements show the storage moduli of $AC_{10}A$ hydrogels in the examined concentration range (below 10%) are typically less than 15% of the values calculated on the basis of an ideal network assumption where 100% chains are elastically effective, suggesting a substantial fraction of looped chains (discussed in Chapter II). The tendency of $AC_{10}A$ chains to form loops and the small aggregation number of the endgroups combine to yield a high probability of forming disengaged clusters as shown in Figure 1. Clusters at the surface diffuse into the surrounding medium, and endgroup exchange among different junction points assures that disengaged clusters are regenerated, leading to relatively rapid dissolution of these physical gels in open systems.

Stabilizing the network in open solutions can be achieved by introducing covalent bonds, such as disulfide bonds, between leucine zippers. Nature provides several examples of protein assemblies stabilized in analogous fashion. Type IV collagen forms a network through formation of twisted triple helices linked by multiple disulfide bonds[20]. Fibrous α-keratin in hair and wool is composed of self-assembled coiled-coils, stabilized by disulfide bonds that contribute to the toughness and abrasion resistance of the structure[21]. Silk fibroin in *Lepidoptera*, from which silk fiber is formed, is composed of three different proteins that are linked by disulfide bonding and hydrophobic interactions[22]. In the systems examined in this work, disulfide bonds are engineered to suppress the generation of disengaged clusters by limiting intramolecular association and by increasing the valency of the building units of the physical gels.

To implement the design proposed above, several considerations must be taken into account. First, the cysteine residues in the leucine zipper domains must be placed

such that they are buried in the hydrophobic core and brought into proximity for disulfide bond formation when the zippers assemble into oligomer bundles. Second, substitution of the residue at the *a* position or at the *d* position by a cysteine residue should cause minimal disruption of the secondary and tertiary structures of the leucine zipper domains. Zhou studied the positional effects of disulfide bonds on leucine zipper stability and found substitution at the *d* position to be most effective[23] for maintaining the secondary structure. Finally, among the six heptad repeats that constitute each coil domain, the specific heptad chosen to bear the newly introduced cysteine residue should favor formation of intermolecular disulfide bonds. The length of a coiled-coil domain with six heptad repeats is 65 Å[17], longer than the average dimension of the midblock. Dynamic light scattering measurements carried out in our laboratory revealed that the midblock chains have an average hydrodynamic diameter of 40 Å (discussed in Chapter II). As a consequence, among looped configurations those with antiparallel association of the leucine zipper endgroups are energetically favored over those with two parallel endgroups, in which the midblock has to be stretched (Figure 2). Therefore, to prevent the cysteine residues in the leucine zipper domains from forming intramolecular disulfide bonds, the cysteine residue in each leucine zipper domain should be engineered asymmetrically. A similar strategy is used to control the orientation specificity of some natural leucine zipper domains: the GCN4 leucine zipper, which bears an asparagine residue positioned asymmetrically, adopts a parallel orientation that enables Asn residues to form interhelical hydrogen bonds; Asn→Leu variants lose orientation specificity[14,24]. On the basis of these considerations, a new triblock protein was designed in which the

leucine residue at the *d* position of the second heptad repeat is substituted by a cysteine residue.

3. Experimental section

3.1. Construction of expression vectors encoding artificial proteins

Scheme 1 illustrates the sequences of the three triblock artificial proteins that will be discussed in this paper. Expression vectors pQE9AC_{10}Acys and pQE9AC_{10}Atrp were constructed previously by Petka[25]. pQE9AC_{10}Acys(L11C) was constructed from pQE9Acys[25] and pQE9C_{10}trp[25] through recombinant DNA manipulation. pQE9Acys(L11C), the L11C mutant of pQE9Acys, was made via the "QuickChange" (Stratagene, La Jolla, CA) procedure using the following oligonucleotides (the mutated codon for the 11th residue in the leucine zipper domain is italicized): 5' C GAA GTG GCC CAG *TGC* GAA AGG GAA GTT AG 3'(sense strand) and 5' CT AAC TTC CCT TTC *GCA* CTG GGC CAC TTC G 3'(antisense strand). The primers were synthesized at the Biopolymer Synthesis Center of the Beckman Institute at the California Institute of Technology. pQE9AC_{10}Acys(L11C) was constructed as follows: DNA segments encoding C_{10} and A(L11C) were excised from pQE9C_{10}trp and pQE9Acys(L11C), respectively, by digestion with *Nhe*I and *Spe*I (New England Biolabs, Beverly, MA). The C_{10} segment was ligated into the *Spe*I site of pQE9Acys(L11C) to yield pQE9AC_{10}cys(L11C). Digestion of pQE9AC_{10}cys(L11C) with *Spe*I followed by ligation with the A(L11C) fragment, gave pQE9AC_{10}Acys(L11C). The sequence of pQE9AC_{10}Acys(L11C) was verified at the DNA sequencing core facility of the Beckman Institute at the California Institute of Technology.

3.2. Protein synthesis and purification

pQE9AC$_{10}$Acys, pQE9AC$_{10}$Atrp and pQE9AC$_{10}$Acys(L11C) were each transformed into *Escherichia coli* strain SG13009, which carries the repressor plasmid pREP4 (Qiagen, Chatsworth, CA). Cultures of SG13009 pQE9AC$_{10}$Acys, SG13009 pQE9AC$_{10}$Atrp and SG13009 pQE9AC$_{10}$Acys(L11C) cells were each grown at 37 °C in 1 L of Terrific Broth (TB) supplemented with 200 mg/L of ampicillin (Sigma, St. Louis, MO) and 50 mg/L of kanamycin (Sigma, St. Louis, MO). The culture was induced with 1.5 mM isopropyl-1-β-D-thiogalactoside (IPTG) (Calbiochem, Inc., San Diego, CA) when it reached an optical density (600 nm) of 0.7 to 1. Protein expression continued for 5 hours; the optical density reached 1.4 to 2. Cells were harvested by centrifugation (5 min, 10,000 g); typical yields were ca. 5 g of wet cell mass per liter of cell culture. The cell pellet was re-suspended in 8 M urea (pH 8.0) and frozen at –80 °C. The thawed lysate was centrifuged at 22,100 g for 20 minutes and the supernatant was collected for purification. A 6×Histidine tag encoded in pQE9 vector allows the protein to be purified by affinity chromatography on a nickel nitrilotriacetic acid resin (Qiagen, Chatsworth, CA) following the denaturing protocol provided by Qiagen. To prevent thiol group oxidation and non-specific disulfide bond formation during purification of AC$_{10}$Acys and AC$_{10}$Acys(L11C), 14 mM β–mercaptoethanol (Sigma, St. Louis, MO) was added to the washing and elution buffers. The eluted fractions were dialyzed against sterile deionized water for three days at room temperature and the proteins were lyophilized. The average protein yield was 85 mg per liter of cell culture.

3.3. Mass spectrometry

AC_{10}Acys and AC_{10}Acys(L11C) were digested by Lys-C, and the resulting proteolytic fragments were analyzed on an Applied Biosystems Voyager mass spectrometer. Purified AC_{10}Acys and AC_{10}Acys(L11C) were dissolved in digestion buffer (25 mM Tris·HCl, pH 8.5, 1 mM EDTA) at a concentration of 0.1 mg/mL. An AC_{10}Acys or AC_{10}Acys(L11C) solution (100 μL) was mixed with 2 μL of 0.1 μg/μL Lys-C (Roche, Palo Alto, CA) and incubated at 37 °C for 6 hours. The reaction was quenched by addition of trifluoroacetic acid (pH<4.0). The sample was then purified on a $ZipTip_{C18}$ column (Millipore, Bedford, MA) and eluted with 10 μL of elution buffer (50% acetonitrile, 50% water, 0.1% trifluoroacetic acid). The MALDI matrix α-cyano-β-hydroxycinnamic acid (4 μL, 10 mg/mL in 50% CH_3CN) was added to 1 μL of purified protein solution, and 0.5 μL of the mixture was spotted on the sample plate and analyzed.

3.4. Free thiol titration

Free thiol concentrations in protein samples were determined by titration with Ellman's reagent[26] (5,5'-dithiobis(2-nitrobenzoic acid), DTNB) (Pierce, Rockford, Illinois). A 10 mM DTNB solution was freshly prepared in 100 mM phosphate buffer or 8 M urea (pH 7.6), supplemented with 1 mM EDTA. Standard titration curves were generated with cysteine hydrochloride monohydrate (Sigma, St. Louis, MO) as the analyte. Each protein solution was mixed with the 10 mM DTNB solution in a volumetric ratio of 9:1, and the reaction mixture was incubated at room temperature for 15 minutes. The free thiol concentration in each protein sample was determined by measuring the absorbance at 412 nm.

3.5. Circular dichroism spectroscopy

CD spectra were recorded at room temperature on an Aviv 62DS spectropolarimeter (Lakewood, NJ). AC_{10}Atrp, AC_{10}Acys and AC_{10}Acys(L11C) solutions (50 μM) were prepared in 100 mM phosphate buffer by weighing at least 3 mg of each protein on a microbalance with an error less than 0.05 mg. Experiments were performed in a rectangular cell with path length of 1 mm. Spectra were scanned from 260 nm to 200 nm with points taken every 0.5 nm. Three scans were performed for each sample and averaged.

3.6. Release studies

Red carboxylate-modified fluorescent polystyrene beads (1 μm) (Molecular Probes, Eugene, OR) were embedded in 6.5% protein gels to a final concentration of 0.01%. Each gel was placed in a chamber filled with 100 mM phosphate buffer (pH 7.6). The volume ratio of buffer to gel was 40:1. The release of the beads and the stability of the gels were monitored using a Zeiss Axiovert 100 fluorescence microscope equipped with a 20×/0.45-NA objective. The illuminating beam for excitation went through a 535 nm bandpass filter, and the fluorescent images were collected through a 565 nm dichromatic splitter and a 610 nm bandpass filter.

Quantitative release rates were measured spectroscopically by using much smaller polystyrene beads (20 nm) that readily dispersed in the aqueous medium above hydrogel layers. For these experiments, hydrogel films with beads embedded were anchored on the interior bottom surfaces of cylindrical vials (12.8 mm diameter). The surfaces of the vials were aminated by cleaning with 98% sulfuric acid (EM Science, Gibbstown, NJ) and

then reacting with a 3-aminopropyltriethoxysilane (Sigma-Aldrich, St. Louis, MO) solution (2%, in ethanol) for 30 minutes, followed by rinsing with ethanol and drying. A protein solution (120 μL, 5.7%, pH 12.0) containing 0.02% red carboxylate-modified fluorescent polystyrene beads (20 nm, Molecular Probes) was added to the treated vial, followed by a pH adjustment with 6 N HCl to yield a pH value of 7.6. The solution gelled, and the final protein concentration was brought to 5.5% with buffer. The vial was placed at the center of a centrifuge holder and centrifuged at 1700 g for two minutes, yielding a flat gel film of 12.8 mm diameter and 0.96 mm thickness. Phosphate buffer (4 mL, pH 7.6, 100 mM) was added into the vial three hours later. The vial was then mounted on an Eppendorf Thermomixer (Brinkmann Instruments, Inc., Westbury, NY) and shaken at 300 rpm. Aliquots (130 μL) of supernatant were taken at successive time points and the fluorescence was measured on a fluorometer (Photon Technology International, Inc., Lawrenceville, NJ). The samples were excited at 575 nm and the emission was scanned from 585 nm to 700 nm. Aliquots were returned into the vial after each measurement to maintain a constant volume of supernatant.

3.7. Particle tracking

Red carboxylate-modified fluorescent polystyrene beads (0.5 μm) (Molecular Probes, Eugene, OR) were embedded in protein solutions at a final concentration of 0.02%. Fluorescence imaging of the embedded beads was performed under epiillumination by using a Zeiss Axiovert 100 microscope equipped with a 100 watt mercury Oriel Q Arc lamp. The illuminating beam for excitation went through a 535 nm bandpass filter. The epifluorescence was collected by using a 40×/1.4-NA oil immersion

Plan Neofluar (Zeiss) objective and imaged through a 565 nm dichromatic splitter and a 610 nm bandpass filter. Images were recorded by a Dage-MTI CCD-72 camera; the analog signal from the camera was converted to a digital movie by a JVC digital video recorder. Digitized movies were analyzed by using a software package written by Crocker and Grier[27]. The software determines particle positions, connects particle positions to form trajectories and determines mean square displacement from those trajectories.

3.8. Multiangle light scattering

A 6% (w/v) AC_{10}Acys(L11C) hydrogel with a pH value of 7.6 was made in 100 mM phosphate buffer. The pH was adjusted to 12.2 twelve hrs later and the solution was converted to a viscous liquid. The solution was transferred into a volumetric flask and the concentration was brought to 4.84×10^{-4} mg/L with 100 mM phosphate buffer (pH 11.0). In order to examine whether the concentration is low enough to allow determination of molecular weight from a Debye plot, a 2.42×10^{-4} mg/L solution was made by diluting the 4.84×10^{-4} mg/L solution. Both solutions were subjected to multiangle light scattering measurements on a DAWN EOS light scattering instrument (Wyatt Technology Corporation, CA). The data were analyzed with Debye plots by using a dn/dc value of 0.185[28].

3.9. Rheological oscillatory shear measurements

AC_{10}Atrp and AC_{10}Acys(L11C) solutions were prepared in phosphate buffer (13 mM $NaH_2PO_4\cdot H_2O$, 87 mM $Na_2HPO_4\cdot 7H_2O$) with their pH values adjusted to 7.0. The

solutions were centrifuged to remove entrapped bubbles before being loaded on an RFS III rheometer (TA instruments, New Castle, Delaware). The temperature was controlled at 22.0 ± 0.1 °C by a peltier thermoelectric device. A parallel-plate geometry (0.5 mm gap and 8 mm diameter) was used for frequency sweep measurements from 100 rad/s to 1 rad/s under a 1% strain, which was confirmed to be within the linear viscoelastic regime on the basis of strain sweep tests. The edge of each sample was covered with mineral oil to minimize solvent evaporation.

3.10. Swelling behavior

AC_{10}Acys(L11C) gel films were made by drying the protein solution (10 μL, 5%, pH 11.0) in a circular reservoir (4.4 mm in diameter) on aminated or untreated glass slides. Re-hydrating the dried pads at neutral pH yielded swollen hydrogel films. The lateral swelling ratio was measured by a micrometer (Mitutoyo). The vertical swelling ratio was measured by analyzing samples containing 0.02% fluorescent beads (0.5 μm, Molecular Probes) on a confocal microscope (Zeiss LSM-Pascal) equipped with a 40× objective. Each sample was scanned in the XY plane and the scanning plane varied in the Z direction with a resolution of 0.2 μm. The thickness of the gel pad was determined by marking the first and the last Z stacks where the embedded fluorescent beads were observed. Dimensional changes in the lateral and vertical directions were also observed through a contact angle goniometer (Ramé-Hart Inc.). The degree of overall swelling was calculated on the basis of the changes in dimension or weight.

3.11. Micropatterning and AFM imaging

Poly(dimethylsiloxane) (PDMS) stamps were prepared as described previously by Jackman et al.[29]. A master consisting of cylindrical photoresist posts supported on a silicon wafer was prepared photolithographically. The posts were 30 μm in diameter, with a center-to-center distance of 60 μm. The height of the posts was controlled to be between 1 and 2 μm. The PDMS (Sylgard 184, Dow Corning, Midland, MI) was cured against the master at 60 °C for 2 hrs and peeled away from the silicon wafer to yield a stamp.

An AC_{10}Acys(L11C) protein solution (2 μL, pH 11.0, 5%) was placed on an aminated glass slide or silicon wafer. A PDMS stamp was placed on the top of the solution with its patterned surface facing down, so that the wells of the PDMS stamp were filled with protein solution and extra solution was squeezed out. After the protein solution dried, the PDMS stamp was peeled from the surface. Dry protein pads on the glass slide or silicon wafer were re-hydrated with aqueous buffer (neutral pH). Micropatterned gel pads were soaked in excess buffer for 48 hrs and the patterns were monitored with a Zeiss optical microscope. Images of the gel pads before and after re-hydration were recorded in tapping mode on a Nanoscope III atomic force microscope (Digital Instruments, Inc.) to examine the changes in size and shape.

4. Results and Discussion

4.1. Protein biosynthesis

AC_{10}Atrp, AC_{10}Acys, and AC_{10}Acys(L11C) were expressed in *E. coli*, purified, and analyzed by SDS-PAGE gel electrophoresis. In order to confirm that the 11th residue

of the leucine zipper domain was mutated from a leucine in AC_{10}Acys into a cysteine in AC_{10}Acys(L11C), proteolytic fragments of purified AC_{10}Acys and AC_{10}Acys(L11C) were prepared by digestion with Lys-C, followed by mass spectral analysis. A point mutation from L to C in the fragment WASGDLENEVAQL(→C)EREVRSLEDEAAELEQK yields an expected shift in mass from 3443.66 Da to 3433.58 Da. The observed fragments appear at 3443.76 Da and 3433.54 Da, respectively, consistent with a single L to C mutation.

4.2. Disulfide bond formation

Disulfide bond formation in 50 μM AC_{10}Acys(L11C) solutions (100 mM phosphate buffer, pH 7.6, room temperature) was analyzed by titration with Ellman's reagent. About 90% of cysteine residues were oxidized within 3 hrs, indicating that no added oxidizing reagent is needed for disulfide bonds to form.

4.3. Secondary structure

AC_{10}Atrp and AC_{10}Acys solutions showed almost identical helicity as evidenced by minima at 222 nm and 208 nm in their circular dichroism spectra. The molar ellipticity of AC_{10}Acys(L11C) at 222 nm was 92% of the values observed for AC_{10}Atrp and AC_{10}Acys (Figure 3), suggesting that the zipper domains remain helical after cysteine residues are incorporated and even after disulfide bonds form. Identical CD spectra were recorded for AC_{10}Acys(L11C) solutions under both oxidizing and reducing conditions, suggesting that it is substitution of the leucine residue by a cysteine residue, rather than disulfide bond formation, that causes this modest disruption of the secondary structure of

the leucine zipper domains. This result also indicates little reaction between C-terminal and internal cysteine residues. Were such linkages significant, the secondary structure of the leucine zipper domain should be highly disrupted, but recoverable under reducing conditions. Fitting the data with a Ridge Regression Analysis (CONTIN) program[30] gives estimates of the percent of α-helix for AC_{10}Acys, AC_{10}Atrp and AC_{10}Acys(L11C) of 34%, 36% and 29% respectively, while the predicted value for AC_{10}Acys and AC_{10}Atrp is 37% if one simply divides the number of amino acids in the putative helical region by the total number of amino acids in the chain. This comparison suggests that ca. 80% helicity is retained in the leucine zipper domains after cysteine residues and disulfide bonds are introduced.

4.4. Encapsulation and release behavior

AC_{10}Acys(L11C) hydrogels showed significantly improved stability compared to AC_{10}Atrp and AC_{10}Acys gels in open solutions, as shown by encapsulation and release of tracer particles. At pH 7.6, none of the fluorescent beads entrapped in AC_{10}Acys(L11C) gels were found to escape into the surrounding buffer after 2 days. In contrast, AC_{10}Atrp and AC_{10}Acys hydrogels dissolved within several hours. Under sterile conditions, AC_{10}Acys(L11C) gels remain stable in open solutions of 100 mM phosphate buffer or Dulbecco's Modified Eagle's Medium (DMEM) for several weeks.

The release rates of embedded beads were quantified by measuring the fluorescence intensity of the surrounding buffer as a function of time. Under oxidizing conditions, no release from the AC_{10}Acys(L11C) gel was observed over several days. For AC_{10}Atrp and AC_{10}Acys gels, release was linear in time (Figure 4), suggesting that

network failure occurred by surface erosion. When placed in reducing buffer (containing 10 mM TCEP), AC_{10}Acys(L11C) gels dissolved rapidly with release of embedded beads (Figure 4). Release from AC_{10}Acys(L11C) gels under reducing conditions was even faster than that from AC_{10}Atrp gels, probably because of the lower helicity and consequent weaker aggregation of the leucine zipper domains in AC_{10}Acys(L11C). This result confirms the important role of disulfide bonds in maintaining the stability of the AC_{10}Acys(L11C) network in open solutions.

4.5. Reversibility in response to pH

Single particle tracking was used to examine the reversibility of gelation of AC_{10}Acys(L11C) in response to pH in closed systems. As shown in Figure 5, the mean square displacement of tracer particles dispersed in a 7.5% AC_{10}Acys(L11C) solution at pH 12.2 increased linearly with time, indicating viscous behavior. When the pH was adjusted from 12.2 to 7.2, the mean square displacement remained essentially constant on a timescale of seconds, consistent with formation of an elastic gel. Viscous behavior was instantly recovered when the pH was returned to 12.2 (Figure 5). As long as the pH was kept at 12.2 only for a short period of time (too short to allow alkaline cleavage of disulfide bonds to become significant[31]), the viscous protein solution gelled again upon acidification. The resulting gel remained stable when placed in open solutions.

Although alkaline cleavage of disulfide bonds can occur at pH 12.2, only about 1% of the cleavage takes place within one hour[31]. Therefore, the instant gel-to-sol transition observed upon raising the pH is attributed to the loss of helical secondary structure in the leucine zipper domains as determined by CD analysis (Figure 6). This

suggests that leucine zipper self-assembly is indispensable in maintaining an AC_{10}Acys(L11C) network even after disulfide bonds form.

According to Miller-Macosko theory[32,33], a network can form from homopolymerization of trifunctional monomers when half of the functional groups have been consumed by intermolecular coupling. Although each AC_{10}Acys(L11C) chain carries three cysteine thiols and more than half form disulfide bonds under the conditions examined here, particle tracking and simple inspection show that the network dissolves when the leucine zipper domains are denatured. Multiangle light scattering measurements (Figure 7) revealed that, upon leucine zipper denaturation at high pH, the disassembled species in the solution are composed of ca. 9 triblock protein chains on average, suggesting that disulfide bonds create predominantly linear linkages rather than trifunctional covalent network junctions. Were such junctions significant, the network structure would be retained after the leucine zippers were denatured. The predominance of linear linkages is most likely due to the redundancy of the disulfide bonds formed from C-terminal cysteine residues.

"Multichains" with predominantly linear linkages created by disulfide bonds act as the building units of AC_{10}Acys(L11C) physical networks. These building units bear many sites of physical association through leucine zipper aggregation. The increased valency of the building units improves the stability of AC_{10}Acys(L11C) hydrogels, while the non-covalent nature of the junctions imparts reversibility to the network. Formation of "multichains" is a consequence of rationally engineered cysteine residues that are positioned in the leucine zipper domains asymmetrically. This design limits intramolecular disulfide bonds and enables chain extension.

We examined directly the possibility that oxidation of cysteine residues in AC_{10}Acys(L11C) could lead to a network in the absence of leucine zipper self-assembly at a concentration of 6% w/v, at which AC_{10}Acys(L11C) solutions form hydrogels under native conditions. A sample of AC_{10}Acys(L11C) with denatured leucine zipper domains and reduced cysteine residues was prepared by dissolving the purified protein (1 mM) in 8 M urea containing 20 mM tris(2-carboxyethyl)phosphine hydrochloride (TCEP), followed by HPLC separation and lyophilization. A solution of the resulting protein was prepared in 8 M urea (pH 7.6) at a concentration of 6% w/v, and the free thiol concentration was titrated at successive time points. As shown in Figure 8, disulfide bond formation was substantially retarded in the absence of the template provided by leucine zipper self-assembly. In solutions containing properly folded zipper domains, 90% of cysteine residues are oxidized after 3 hrs of exposure to ambient air. In urea solutions, however, 90% oxidation requires ca. 60 hrs. Significantly, urea solutions of AC_{10}Acys(L11C) remained fluid even after oxidation, indicating that disulfide bonds alone do not lead to a network in the absence of leucine zipper self-assembly at 6% w/v. The most likely explanation for the absence of gelation is the formation of a significant number of intramolecular disulfide bonds in the random coil protein molecules in the absence of secondary structure.

4.6. Storage modulus

AC_{10}Acys(L11C) hydrogels exhibited higher storage moduli than AC_{10}Atrp hydrogels at the same concentration (Figure 9). The storage modulus of the AC_{10}Acys(L11C) hydrogel increased by ca. 30% in the first hour after preparation, while that of the AC_{10}Atrp hydrogel remained constant. These differences likely reflect the

consequences of placing cysteine residues asymmetrically in the leucine zipper domains. This design allows intramolecular, antiparallel leucine zipper dimers to undergo strand exchange until they form intermolecular coiled coils fastened by disulfide bonds. Reduction in the number of intramolecular loops in the AC_{10}Acys(L11C) hydrogel leads to a higher storage modulus.

4.7. Swelling behavior

AC_{10}Acys(L11C) gel pads anchored on aminated glass surfaces undergo anisotropic swelling, which was observed through the microscope of a contact angle goniometer. Quantitative measurements by confocal microscopy revealed that the lateral swelling ratio was very slight (close to 1) while the vertical swelling ratio was as high as 6 (Figure 10). When AC_{10}Acys(L11C) gel pads were made on untreated glass surfaces, they detached from the surface upon hydration. The lateral swelling ratio of unconstrained gels was approximately twice that of anchored gels (Figure 10). This suggests that the amine groups on the treated surface play an important role in anchoring the gel pad and suppressing lateral swelling. Since the midblock of AC_{10}Acys(L11C) carries 10 glutamic acid residues and is therefore negatively charged at pH 7.6, anchoring of the gels is likely to occur through electrostatic attraction.

The overall swelling ratio of an unconstrained AC_{10}Acys(L11C) gel pad in 100 mM phosphate buffer (pH 7.6) is 18.9±2.3, as calculated on the basis of the change in weight. Calculation on the basis of dimensional change reveals an overall swelling ratio of 17.2±2.6, reasonably consistent with the value obtained from gravimetric measurements. Although the vertical swelling of an unconstrained gel is less than that of

an anchored gel, the overall swelling of the unconstrained gel (about 18) is much greater than that of the anchored gel (about 6). This accords with prior studies of anisotropic swelling of synthetic gels constrained on substrates[34,35]. For constrained gels, the lateral stress imposed by the substrate complements the elastic force in balancing the osmotic pressure, and thereby reduces the overall degree of swelling.

4.8. Micropatterning

The reversibility of gelation in response to pH in closed systems, the stability of the gels in open solutions, and the anisotropic swelling of the gels on aminated surfaces allowed us to generate stable AC_{10}Acys(L11C) hydrogel micropatterns by soft lithography. Protein solutions of low viscosity were prepared at high pH, and then subjected to soft lithographic micropatterning as described in the experimental section. Re-hydration of the dried protein at neutral pH resulted in micropatterned gel pads. The diameter of the gel pads was consistent with that of the wells of the stamp (30 μm), and remained constant when the gel pads were placed in excess buffer for 48 hrs, as examined by light microscopy. Further examination by AFM showed no obvious change in shape within 24 hrs (Figure 11). Retention of the original micropatterns is facilitated by electrostatic attraction between the gel pads and the aminated surface, which not only immobilizes the gel pads, but also suppresses their swelling in the lateral direction. The ability of the hydrogel pads to retain shape and registration is important for their potential application in array technologies.

5. Conclusions

Artificial protein hydrogels were assembled through the combined effects of leucine zipper self-assembly and disulfide bonding. These hydrogels retain their integrity in open solutions for several weeks, and exhibit reversibility of gelation in response to pH in closed systems. Gel pads made on aminated surfaces undergo anisotropic swelling, with lateral swelling significantly suppressed. The reversibility, stability, and anisotropic swelling allow the generation of stable hydrogel micropatterns through soft lithography. These hydrogels show promise with respect to application in controlled release and microarray technologies, and their potential as scaffold matrices for tissue engineering is being addressed by ongoing studies.

6. References

(1) Lee, K. Y.; Mooney, D. J. *Chemical Reviews* **2001**, *101*, 1869-1879.

(2) Gutowska, A.; Jeong, B.; Jasionowski, M. *Anatomical Record* **2001**, *263*, 342-349.

(3) Delgado, M.; Spanka, C.; Kerwin, L. D.; Wentworth, P.; Janda, K. M. *Biomacromolecules* **2002**, *3*, 262-271.

(4) Halstenberg, S.; Panitch, A.; Rizzi, S.; Hall, H.; Hubbell, J. A. *Biomacromolecules* **2002**, *3*, 710-723.

(5) Hisano, N.; Morikawa, N.; Iwata, H.; Ikada, Y. *Journal of Biomedical Materials Research* **1998**, *40*, 115-123.

(6) Jen, A. C.; Wake, M. C.; Mikos, A. G. *Biotechnology and Bioengineering* **1996**, *50*, 357-364.

(7) Risbud, M.; Endres, M.; Ringe, J.; Bhonde, R.; Sittinger, M. *Journal of Biomedical Materials Research* **2001**, *56*, 120-127.

(8) Stile, R. A.; Healy, K. E. *Biomacromolecules* **2001**, *2*, 185-194.

(9) Martens, P. J.; Bryant, S. J.; Anseth, K. S. *Biomacromolecules* **2003**, *4*, 283-292.

(10) Petka, W. A.; Harden, J. L.; McGrath, K. P.; Wirtz, D.; Tirrell, D. A. *Science* **1998**, *281*, 389-392.

(11) Wang, C.; Stewart, R. J.; Kopecek, J. *Nature* **1999**, *397*, 417-420.

(12) Surks, H. K.; Richards, C. T.; Mendelsohn, M. E. *Journal of Biological Chemistry* **2003**, *278*, 51484-51493.

(13) O'Shea, E. K.; Rutkowski, R.; Stafford, W. F.; Kim, P. S. *Science* **1989**, *245*, 646-648.

(14) O'Shea, E. K.; Klemm, J. D.; Kim, P. S.; Alber, T. *Science* **1991**, *254*, 539-544.

(15) Ishiyama, M.; Shiga, M.; Sasamoto, K.; Mizoguchi, M.; He, P. G. *Chemical & Pharmaceutical Bulletin* **1993**, *41*, 1118-1122.

(16) Xu, B.; Yekta, A.; Li, L.; Masoumi, Z.; Winnik, M. A. *Colloids and Surfaces a-Physicochemical and Engineering Aspects* **1996**, *112*, 239-250.

(17) Kennedy, S. B.; Ph.D. Dissertation; University of Massachusetts Amherst: Amherst, MA 2001.

(18) Chao, H. M.; Houston, M. E.; Grothe, S.; Kay, C. M.; OconnorMcCourt, M.; Irvin, R. T.; Hodges, R. S. *Biochemistry* **1996**, *35*, 12175-12185.

(19) Wendt, H.; Berger, C.; Baici, A.; Thomas, R. M.; Bosshard, H. R. *Biochemistry* **1995**, *34*, 4097-4107.

(20) Kuhn, K.; Glanville, R. W.; Babel, W.; Qian, R. Q.; Dieringer, H.; Voss, T.; Siebold, B.; Oberbaumer, I.; Schwarz, U.; Yamada, Y. *Annals of the New York Academy of Sciences* **1985**, *460*, 14-24.

(21) Yu, J. L.; Yu, D. W.; Checkla, D. M.; Freedberg, I. M.; Bertolino, A. P. *Journal of Investigative Dermatology* **1993**, *101*, S56-S59.

(22) Inoue, S.; Tanaka, K.; Arisaka, F.; Kimura, S.; Ohtomo, K.; Mizuno, S. *Journal of Biological Chemistry* **2000**, *275*, 40517-40528.

(23) Zhou, N. E.; Kay, C. M.; Hodges, R. S. *Biochemistry* **1993**, *32*, 3178-3187.

(24) Lumb, K. J.; Kim, P. S. *Biochemistry* **1995**, *34*, 8642-8648.

(25) Petka, W. A.; Ph.D. Dissertation; University of Massachusetts Amherst: Amherst, MA 1997.

(26) Riddles, P. W.; Blakeley, R. L.; Zerner, B. *Methods in Enzymology* **1983**, *91*, 49-60.

(27) Crocker, J. C.; Grier, D. G. *Journal of Colloid and Interface Science* **1996**, *179*, 298-310.

(28) Huglin, M. B. *Light scattering from polymer solutions*; Academic Press: London, New York, 1972.

(29) Jackman, R. J.; Duffy, D. C.; Ostuni, E.; Willmore, N. D.; Whitesides, G. M. *Analytical Chemistry* **1998**, *70*, 2280-2287.

(30) Provencher, S. W.; Glockner, J. *Biochemistry* **1981**, *20*, 33-37.

(31) Kuramitsu, S.; Hamaguchi, K. *Journal of Biochemistry* **1979**, *85*, 443-456.

(32) Miller, D. R.; Macosko, C. W. *Macromolecules* **1976**, *9*, 206-211.

(33) Macosko, C. W.; Miller, D. R. *Macromolecules* **1976**, *9*, 199-206.

(34) Tanaka, T.; Sun, S. T.; Hirokawa, Y.; Katayama, S.; Kucera, J.; Hirose, Y.; Amiya, T. *Nature* **1987**, *325*, 796-798.

(35) Harmon, M. E.; Tang, M.; Frank, C. W. *Polymer* **2003**, *44*, 4547-4556.

Scheme 5.1. Schematic representations and amino acid sequences of triblock proteins and their constituent domains

Leucine zipper A  **SGDLENE VAQLERE VRSLEDE AAELEQK VSRLKNE IEDLKAE**

mid-block C_{10}  **$[AGAGAGPEG]_{10}$**

A(L11C)  **SGDLENE VAQCERE VRSLEDE AAELEQK VSRLKNE IEDLKAE**

AC_{10}Acys 

MRGSHHHHHHGSDDDDKWA **SGDLENE VAQLERE VRSLEDE AAELEQK VSRLKNE IEDLKAE** IGDHVAPRDTSYRDPMG **$(AGAGAGPEG)_{10}$**ARMPT **SGDLENE VAQLERE VRSLEDE AAELEQK VSRLKNE IEDLKAE** IGDHVAPRDTSMGGC

AC_{10}Atrp 

MRGSHHHHHHGSDDDDKA **SGDLENE VAQLERE VRSLEDE AAELEQK VSRLKNE IEDLKAE** IGDHVAPRDTSYRDPMG **$(AGAGAGPEG)_{10}$**ARMPT **SGDLENE VAQLERE VRSLEDE AAELEQK VSRLKNE IEDLKAE** IGDHVAPRDTSW

AC_{10}Acys (L11C) 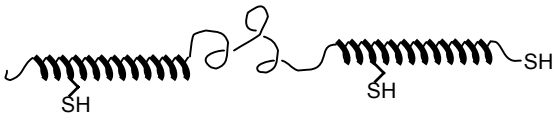

MRGSHHHHHHGSDDDDKWA **SGDLENE VAQCERE VRSLEDE AAELEQK VSRLKNE IEDLKAE** IGDHVAPRDTSYRDPMG **$(AGAGAGPEG)_{10}$**ARMPT **SGDLENE VAQCERE VRSLEDE AAELEQK VSRLKNE IEDLKAE** IGDHVAPRDTSMGGC

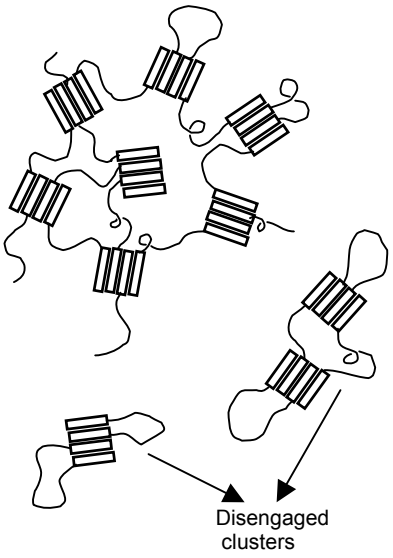

Figure 5.1. Disengaged clusters form constantly in $AC_{10}A$ hydrogels, causing dissolution.

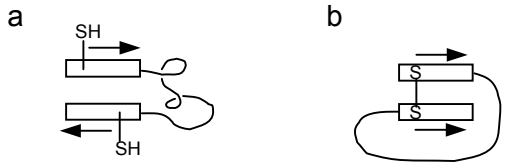

Figure 5.2. Rationale for asymmetric placement of the cysteine residue. (a) Looped configurations predominantly involve antiparallel association of leucine zipper endgroups; asymmetric placement of the cysteine residue disfavors disulfide linkages in this configuration. (b) Only in the rare event of loop formation with parallel endgroups would an intramolecular disulfide bond form.

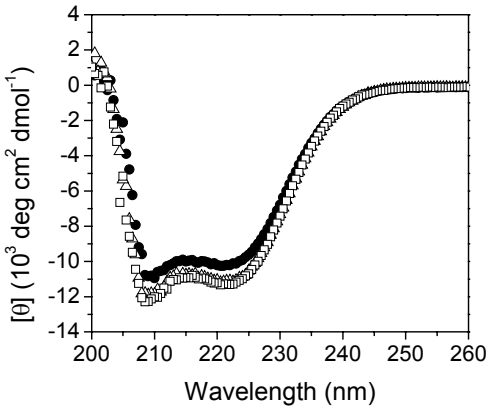

Figure 5.3. CD spectra of 50 μM artificial protein solutions (pH 7.6, room temperature, 100 mM phosphate buffer).

△ AC_{10}Acys; □ AC_{10}Atrp; ● AC_{10}Acys(L11C).

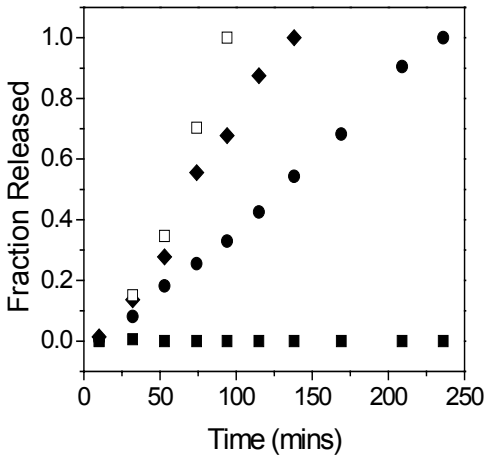

Figure 5.4. Release of embedded fluorescent beads (20 nm) from hydrogel films made from different proteins (5.5% w/v, pH 7.6, room temperature, 100 mM phosphate buffer).

■ AC_{10}Acys(L11C); ● AC_{10}Acys; ◆ AC_{10}Atrp; □ AC_{10}Acys(L11C) in reducing buffer (10 mM TCEP).

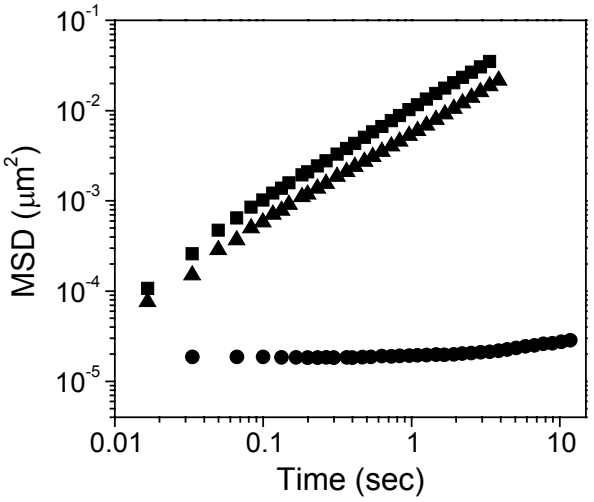

Figure 5.5. Mean square displacement of beads (500 nm) embedded in 7.5% AC_{10}Acys(L11C) solutions (room temperature, 100 mM phosphate buffer). ■ pH 12.2; ● pH adjusted from 12.2 to 7.2; ▲ pH adjusted from 12.2 to 7.2, and adjusted back to 12.2 three hours later.

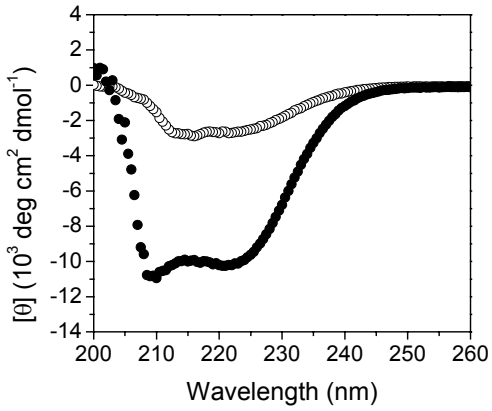

Figure 5.6. CD spectra of 50 μM AC_{10}Acys(L11C) solutions at different pH values (room temperature, 100 mM phosphate buffer). ● pH 7.6; ○ pH 12.2. Percentages of α helix at pH 7.6 and 12.2 are estimated as 29% and 3%, respectively by a Ridge Regression Analysis (CONTIN) program[30].

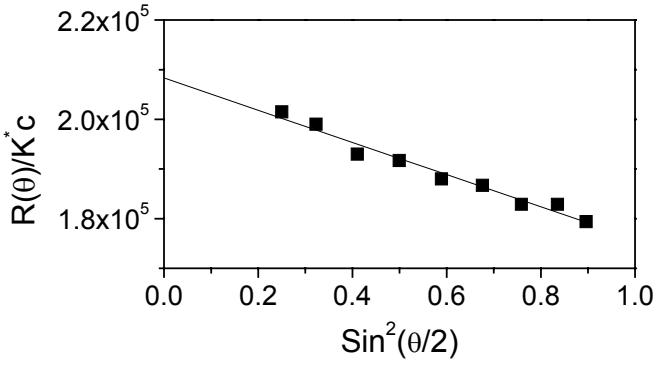

Figure 5.7. Debye plot of multiangle light scattering signals from a 2.42×10^{-4} mg/L solution (room temperature, pH=11.0) reveals that the average molecular weight of the clusters disassembled from an AC_{10}Acys(L11C) hydrogel at pH 12.2 is ca. 207,300. This corresponds to ca. 9 chains in each cluster. (The molecular weight of each AC_{10}Acys(L11C) chain is 22,433.)

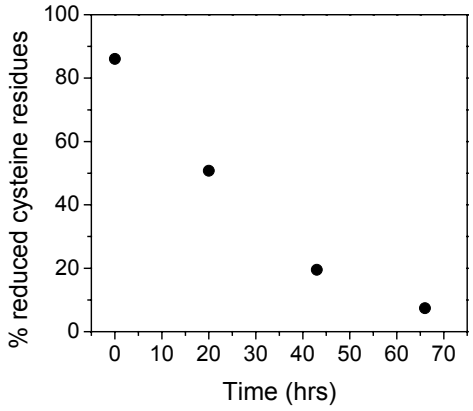

Figure 5.8. Percentage of reduced cysteine residues in a 6% w/v AC_{10}Acys(L11C) solution in 8 M urea as a function of time (pH 7.6, room temperature). The dry protein was pretreated so that the leucine zipper domains were denatured and the majority of the cysteine residues were reduced.

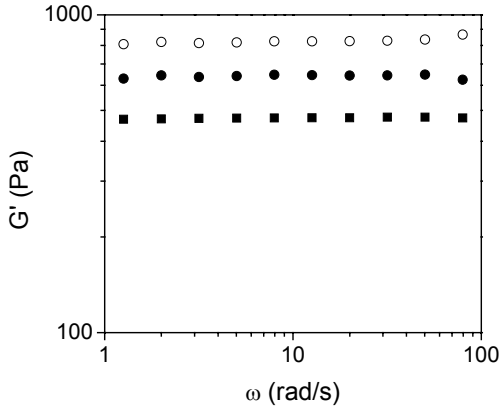

Figure 5.9. Storage moduli of protein hydrogels as determined by rheological oscillatory frequency sweep tests (7% w/v, 100 mM phosphate buffer, pH 7.0, 22 °C, 1% strain). ■ AC_{10}Atrp; ● ○ AC_{10}Acys(L11C) (closed symbols, measured immediately after preparation of the gel; open symbols, measured 1 hr later).

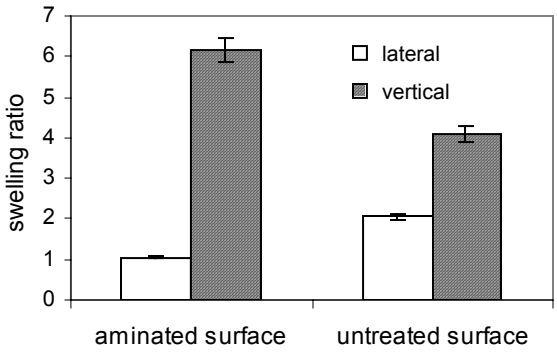

Figure 5.10. Lateral and vertical swelling ratios of AC_{10}Acys(L11C) gels on aminated and untreated surfaces. (the diameter to thickness aspect ratio of the dry protein pad is ca. 150)

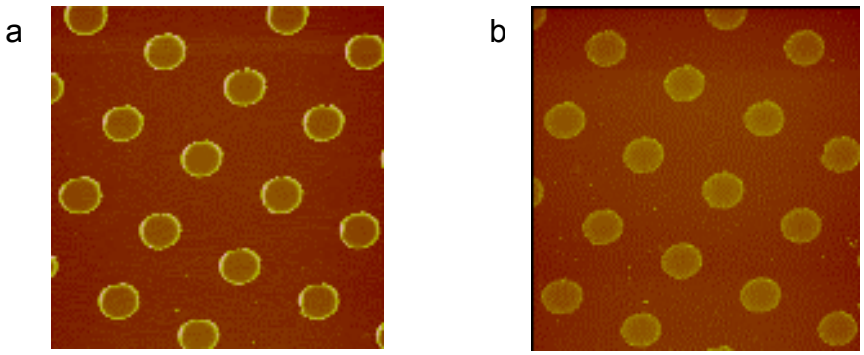

Figure 5.11. Atomic force images of micropatterned AC10Acys(L11C) gel pads acquired in tapping mode (100 μm×100 μm). (a) before re-hydration (b) after 24 hrs of re-hydration in excess water. The image was recorded after the gel pads were re-dried. No obvious loss of material or change in shape was observed.